



Since January 2020 Elsevier has created a COVID-19 resource centre with free information in English and Mandarin on the novel coronavirus COVID-19. The COVID-19 resource centre is hosted on Elsevier Connect, the company's public news and information website.

Elsevier hereby grants permission to make all its COVID-19-related research that is available on the COVID-19 resource centre - including this research content - immediately available in PubMed Central and other publicly funded repositories, such as the WHO COVID database with rights for unrestricted research re-use and analyses in any form or by any means with acknowledgement of the original source. These permissions are granted for free by Elsevier for as long as the COVID-19 resource centre remains active.



Pulmonary high-resolution computed tomography findings in nephropathia epidemica

Antti Paakkala^{a,*}, Ritva Järvenpää^a, Satu Mäkelä^{b,c}, Heini Huhtala^d, Jukka Mustonen^{b,c}

^a Medical Imaging Centre, Tampere University Hospital, 33521 Tampere, Finland

^b Department of Internal Medicine, Tampere University Hospital, 33521 Tampere, Finland

^c Medical School, University of Tampere, 33521 Tampere, Finland

^d School of Public Health, University of Tampere, 33521 Tampere, Finland

ARTICLE INFO

Article history:

Received 9 January 2011

Accepted 21 April 2011

Keywords:

High-resolution computed tomography
Hantavirus pulmonary syndrome
Nephropathia epidemica
Puumala virus

ABSTRACT

Purpose: To evaluate lung high-resolution computed tomography (HRCT) findings in patients with Puumala hantavirus-induced nephropathia epidemica (NE), and to determine if these findings correspond to chest radiograph findings.

Materials and methods: HRCT findings and clinical course were studied in 13 hospital-treated NE patients. Chest radiograph findings were studied in 12 of them.

Results: Twelve patients (92%) showed lung parenchymal abnormalities in HRCT, while only 8 had changes in their chest radiography. Atelectasis, pleural effusion, intralobular and interlobular septal thickening were the most common HRCT findings. Ground-glass opacification (GGO) was seen in 4 and hilar and mediastinal lymphadenopathy in 3 patients. Atelectasis and pleural effusion were also mostly seen in chest radiographs, other findings only in HRCT.

Conclusion: Almost every NE patient showed lung parenchymal abnormalities in HRCT. The most common findings of lung involvement in NE can be defined as accumulation of pleural fluid and atelectasis and intralobular and interlobular septal thickening, most profusely in the lower parts of the lung. As a novel finding, lymphadenopathy was seen in a minority, probably related to capillary leakage and overall fluid overload. Pleural effusion is not the prominent feature in other viral pneumonias, whereas intralobular and interlobular septal thickening are characteristic of other viral pulmonary infections as well. Lung parenchymal findings in HRCT can thus be taken not to be disease-specific in NE and HRCT is useful only for scientific purposes.

© 2011 Elsevier Ireland Ltd. All rights reserved.

1. Introduction

Nephropathia epidemica (NE) is a mild type of hemorrhagic fever with renal syndrome (HFRS), caused by Puumala virus [1]. The virus is a member of the Hantavirus genus in the Bunyaviridae family and is carried by bank voles (*Myodes glareolus*) [1]. NE is prevalent in Scandinavia, European Russia, Balkans, and also in many parts of Western Europe [1]. Approximately 1000–3000 serological diagnoses of Puumala virus infection are made in Finland annually, and the seroprevalence in the population is 5% [2]. Other Hantaviruses causing HFRS include Hantaan, Dobrava, Saaremaa, and Seoul viruses; while in the Americas, Sin Nombre, Andes, and

Black Creek Canal viruses cause Hantavirus cardiopulmonary syndrome (HCPS) [1].

NE is often referred to as a mild form of HFRS. It is characterized by acute fever, head and backache; hemorrhages are rare. Respiratory tract symptoms or findings have been recorded in about one fifth of patients [3]. An increase in serum creatinine concentration, hematuria and proteinuria, thrombocytopenia, hypoproteinemia and moderately elevated leukocyte count and C-reactive protein values are typical laboratory findings [3–5]. Acute renal failure (ARF) is evident in over 90% of hospital-treated patients [3]. Oliguria or anuria is seen in 54% and 8% respectively, followed by polyuria and spontaneous recovery [4].

Abnormalities in chest radiographs have previously been reported in 16–53% of NE patients [3,4,6–8]. Pleural effusion, atelectasis and interstitial infiltrates are the most common chest radiograph findings [6–8]. In contrast to intralobular and interlobular septal thickening and centrilobular nodules, pleural effusion is not the prominent feature in other viral pneumonias (Table 1)

* Corresponding author. Tel.: +358 3 31169347; fax: +358 3 31165586.

E-mail addresses: antti.paakkala@pshp.fi (A. Paakkala), ritva.jarvenpaa@pshp.fi (R. Järvenpää), satu.marjo.makela@uta.fi (S. Mäkelä), heini.huhtala@uta.fi (H. Huhtala), jukka.mustonen@uta.fi (J. Mustonen).

Table 1
Summary of HRCT findings in viral pneumonias [9].

Cause of pneumonia	Centrilobular nodules	Ground-glass attenuation with or without lobular distribution	Segmental consolidation attenuation	Diffuse ground-glass
Influenza virus	+++	+++	+	+
Measles virus	++	+	+	+
Epstein-Barr virus	+	+	+	+
Adenovirus	++	+	+++	
Herpes simplex virus	+	+++		
Varicella-zoster virus	+++	+		
SARS (coronavirus)	+	+++	++	+

Plus signs indicate the relative frequency of the findings from lowest (+) to highest (+++). SARS (severe acute).

[9]. In addition to the degree of ARF and fluid retention, the occurrence and severity of findings have been found to be associated with hypoproteinemia and leukocytosis, which suggests that capillary leakage and inflammation may play a role in NE lung involvement [7,8,10,11].

In a Swedish prospective study of 19 patients with acute NE, computed tomography (CT) showed pulmonary infiltrates and/or pleural effusion in 10 patients [6]. Recently, Fakhrai et al. [12] reported one NE patient who presented with interstitial edema with thickening of the interlobular septa, peribronchial cuffing, ground-glass opacities (GGO), and small pleural and pericardial effusions on the CT.

Puumala virus is genetically closely related to Sin Nombre virus, which causes HCPS [13–15]. Radiologically HCPS is characterized by acute respiratory distress syndrome, non-cardiogenic perihilar pulmonary edema and bilateral interstitial and alveolar infiltrates with pleural effusions [16]. The histological picture is characterized by interstitium and airspace edema, mild to moderate interstitial infiltrates of lymphocytes, and epithelial necrosis with destruction of alveolar pneumocytes and hyaline membranes [15]. Two case reports about high-resolution computed tomography (HRCT) findings in HCPS were published [17,18]. HRCT demonstrated extensive bilateral GGO most severe in the middle and lower lung zones. Also noted were a few slightly thickened interlobular septa, a few poorly defined small nodules, bronchial wall thickening and small bilateral pleural effusion [17]. In the other case report “crazy paving” pattern was also seen [18].

To the best of our knowledge, HRCT findings have not previously been systematically studied in NE or in other HFRS diseases. In order to evaluate the mechanisms of abnormalities in lung parenchyma, we studied the lung HRCT findings in 13 patients and compared them to the chest radiograph findings.

2. Materials and methods

2.1. Participants

A total of 13 hospitalized patients with serologically confirmed [19] acute Puumala virus infection were studied. The cohort comprised 10 males and 3 females, aged from 31 to 67 (mean 45) years. Three of the patients had one or more of the following chronic diseases: sick sinus syndrome, atrial fibrillation, type two diabetes mellitus and bronchial asthma. The median duration of symptoms of NE before hospital admission was 4 (range 2–7) days. The median time of hospitalization was 4 (range 3–14) days. The patients had a typical clinical course of NE (Table 2). One patient needed transient dialysis treatment. Written consent was required. The study was approved by the Ethics Committee of Tampere University Hospital, and the research was conducted according to the principles of the Declaration of Helsinki.

2.2. Chest radiography

Digital posteroanterior and lateral chest radiographs were evaluated by two experienced chest radiologists with agreement by consensus. They were unaware of the patients' clinical data. All patients' chest radiographs were analyzed first and findings were registered, HRCT images were evaluated immediately thereafter. Evaluations were made with an Advantage Windows 4.3 workstation (General Electric Medical Systems, Paris). The nature and location of the abnormalities in chest radiographs were analyzed in 6 fields of the lung, the low, middle and upper fields of the right and left lung separately. The findings (Table 3) were graded as normal or abnormal.

2.3. HRCT technique

HRCT studies were performed with a multislice scanner (GE Light speed 16 Advantage; GE Healthcare, Milwaukee; WI, USA). Images were obtained during full inspiration in supine position. The slice thickness was 1.25 mm. The slices were taken at 20 mm intervals from the lung apex to the costophrenic angle. The imaging parameters were 120 kV and 160 mA. The reconstruction kernel was “lung”. The window settings were appropriate for viewing the lung parenchyma (W1500, L-500) and soft tissues (W400, L70). Data analysis was carried out using SPSS statistical software (version 14.0, SPSS Inc., Chicago, IL). The findings (Table 3) were graded as normal or abnormal. Maximum level of pericardium and pleural fluid were measured.

3. Results

3.1. HRCT findings

HRCT examinations were performed on admission to the hospital, which was 7 (median) days (range 4–16) from onset of symptoms of NE. Twelve out of 13 (92%) patients had abnormalities in their HRCT (Table 3). Atelectasis was seen in 11, bilaterally in 10 patients, present in the lower lobes on both sides. Pleural effusion was seen in 9, bilaterally in 7 patients (Fig. 1). The median amount of pleural effusion was on the right side 21 (range 7–29) mm and on the left 16 (range 10–33) mm. Intralobular and interlobular septal thickening were seen in 7 and GGO in 4 patients, most profusely in the lower parts of the lung (Fig. 2). Bronchial wall thickening was seen in 2 patients. Hilar and mediastinal lymphadenopathy was seen in 3 patients (minimal lymph node transverse length >10 mm). One patient had slightly enlarged heart size and 2 had pericardial fluid (5 mm and 9 mm). None had visually increased venous stasis. No interstitial or alveolar edema was seen.

Table 2
Clinical and laboratory findings in 13 patients with acute NE.

	Median	Range	Reference values
Change in body weight ^a (kg) 4.0–12.0	4.0	0–12.0	
Max. blood leukocyte count (10 ⁹ /l)	10.0	8.8–25.7	3.4–8.2
Max. plasma C-reactive protein (mg/l)	85	27–154	<10
Max. serum creatinine (μmol/l)	384	43–1499	<105 in men, <90 in women
Min. blood platelet count (10 ⁹ /l)	61	9–115	150–360

^a Difference between highest and lowest weight during hospital care. Change in weight reflects fluid retention during the oliguric phase. The highest and the lowest value of each patient of the various variables measured during hospitalization were designated as the maximum and minimum values.

Table 3
HRCT and chest radiograph findings in 13 patients with acute NE.

HRCT findings										Chest radiograph findings	
PN	IIST	GGO	BWT	Atelectasis	Pl effusion	Adenopathy	EH	PFTI	TI	Atelectasis	Pl effusion
1	–	–	–	+	+	–	–	–	3	+	+
2	–	–	–	+	–	–	–	–	2	+	–
3	+	–	+	–	–	–	–	–	0	–	–
4	–	–	–	+	+	+	+	+	3	+	–
5	+	–	–	+	+	–	–	–	2	+	+
6	–	–	–	–	–	–	–	–	1	–	–
7	–	+	–	+	+	–	–	–	3	+	+
8	+	–	–	+	+	–	–	–	1	+	+
9	+	+	–	+	+	–	–	–	2	–	–
10	+	+	–	+	–	–	–	–	1	–	–
11	+	+	+	+	+	+	–	+	6	+	+
12	+	–	–	+	+	+	–	–	2	–	+
13	–	–	–	+	+	–	–	–		NA	NA

Plus signs indicate yes, minus no. Abbreviations: PN = patient number, IIST = intralobular and interlobular septal thickening, GGO = ground-glass opacification, BWT = bronchial wall thickening, Pl = pleural, EH = enlarged heart, PF = pericardial fluid, TI = time interval between HRCT study and chest radiograph (days), NA = not available.

3.2. Chest radiograph findings

Chest radiography was undertaken in 12 cases. The time interval between chest radiograph and HRCT study was a median 2 (range 0–6) days (Table 3). Eight out of 12 (67%) patients showed abnormalities in their chest radiography. Atelectasis and pleural effusion were seen in 5, 2 had only atelectasis and 1 only pleural fluid. Three patients evincing changes in their HRCT were graded as normal based on chest radiography. If atelectasis or pleural fluid were seen in HRCT, they also were found in chest radiography in most cases. Three patients' atelectasis and 2 patients' pleural effusion were not

seen in chest radiography. No intralobular and interlobular septal thickening or GGO was seen in chest radiographs, likewise no hilar and mediastinal lymphadenopathy.

4. Discussion

Radiological findings in lung HRCT of NE patients are here described and the relation to chest radiographs is discussed.

Viruses are the major cause of respiratory tract infection in the community. The epithelial lining of the various parts of the respiratory tract is the main target, tracheobronchitis, bronchiolitis, and pneumonia being thus the main manifestations of viral infection [9]. In one study where the pathogenetic mechanisms underlying pulmonary involvement in NE were investigated, the findings suggested that pulmonary involvement might be the inherent trait of NE [20]. Although Puumala virus is pantropic, i.e. it can infect a

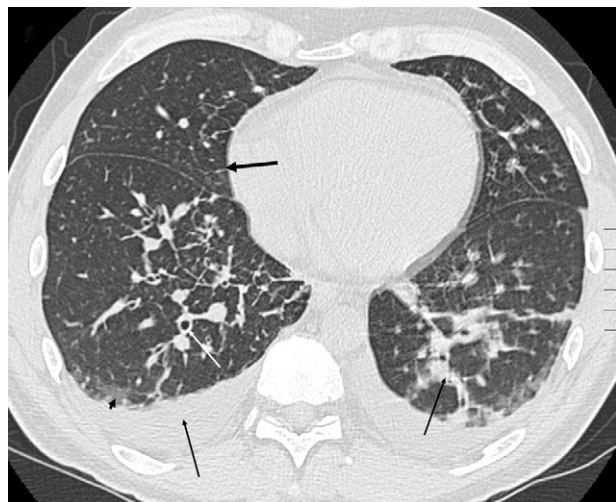


Fig. 1. HRCT of the lungs on the 8th day from the onset of symptoms. Pleural effusion was bilateral and atelectasis was seen in lower lobe on the left side (straight arrows). Intralobular and interlobular septal thickening were seen bilaterally (thick arrow). GGO was seen most profusely in the lower parts of the lung (arrowhead). This patient had also bronchial wall thickening (straight white arrow). Most of the patients had ventilation artifacts because of bad condition.

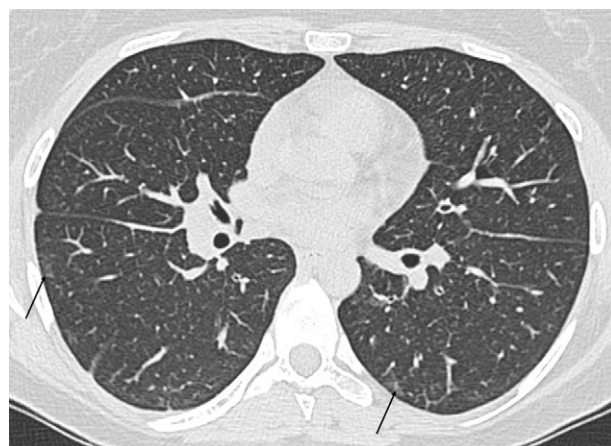


Fig. 2. HRCT of the lungs on the 8th day from the onset of symptoms. GGO was seen most profusely in the lower parts of the lung (arrows).

wide variety of human cells, including cells originating from brain, heart, lung, spleen, liver and kidney tissue, its primary replication site seems to be in the lungs [21].

The pathologic course of viral pneumonia begins with destruction and sloughing of respiratory ciliated, goblet and mucous cells [22]. The bronchial and bronchiolar walls together with the interstitial septa of the lungs become thickened owing to edema and inflammatory cells, primarily lymphocytes. This so-called interstitial pneumonitis is often patchy, affecting predominantly the peribronchial portions of the lobules. With more severe inflammation the alveoli fill with inflammatory exudates, which may be hemorrhagic, and hyaline membranes may form. As Puumala virus infects endothelial cells *in vitro* with no visible changes in the cell morphology, it is possible that immunological mechanisms also contribute to the endothelial damage or functional changes, leading to capillary leakage [23].

Imaging findings of viral pneumonia do not usually allow the diagnosis of a specific virus infection. Nevertheless, the combination of HRCT features varies somewhat among individual viral pneumonias (Table 1) [9]. In the present study pleural effusion and atelectasis were the most common HRCT findings, which coincidence with our previous chest radiograph findings [7,8]. Pleural effusion is not the prominent feature in viral pneumonia, although small effusions do not rule out the diagnosis. Pleural effusion often causes basal atelectasis, in our study only two patients had atelectasis apart from effusion. In HRCT pleural effusion is easy to detect; it is reported that the minimum pleural fluid volume detectable on standing posteroanterior radiographs is 175 ml [24]. In a study with 10-dengue hemorrhagic fever patients who underwent sonography and chest radiography, sonography detected pleural effusion in all 10, whereas radiography detected it only in 3 cases [25]. Accumulation of pleural fluid in acute NE could reflect fluid retention due to ARF, but might also be taken as a sign of capillary leakage [7].

In the present study, 12 patients (92%) showed changes in their lung HRCT, which is more than previously reported with chest radiography [3,4,6–8]. To the best of our knowledge, lung HRCT findings have not previously been systematically studied in NE. CT scans and chest radiographs of the lungs have been examined in a Swedish prospective study involving 19 patients with acute NE [6]. CT revealed pulmonary infiltrates and/or pleural effusion in 10 (53%) patients and in 2 of them abnormalities were shown only by CT [6]. Patients with pathologic lung findings evinced a more pronounced inflammatory response, as measured by CRP and blood leukocyte count, than did those yielding normal findings. HRCT is more accurate than CT and much more accurate than chest radiography, and parenchymal findings are easier to detect with HRCT, which would explain the difference.

In the present study intralobular and interlobular septal thickening were seen in 54% and GGO in 31% of patients in HRCT examination. In our previous study chest radiography showed interstitial infiltrates in only 16% of 344 NE patients [8]. We assume that the interstitial infiltrates previously seen in NE patient chest radiographs are the same finding as intralobular and interlobular septal thickening in HRCT. Also in the present study HRCT parenchymal findings, intralobular and interlobular septal thickening or GGO, were not seen in chest radiographs. In the previous case report about HRCT findings in HCPS, chest radiograph showed minimal bilateral hazy increased opacification and small bilateral pleural effusion but HRCT demonstrated extensive bilateral GGO and also few slightly thickened interlobular septa, a few poorly defined small nodules, bronchial wall thickening and small bilateral pleural effusion [17]. In the other case report “crazy paving” pattern was also seen [18], such kind of finding was not seen in our study. Septal thickening is early stage finding in interstitial edema and GGO can be seen in alveolar edema, otherwise typical pulmonary edema findings were not seen in our study.

In our previous study with 70 NE cases chest radiography revealed slight cardiac enlargement in 3 patients [26]. Echocardiography was performed in 43 of 70 patients, of who 6 showed left ventricular contraction abnormalities and 1 pericardial effusion. In the present study 1 patient had a slightly enlarged heart and 2 had slight amounts of pericardial fluid. However, no venous congestion was evident in these patients. It has previously been thought possible that venous congestion could be the sole or coexisting cause of findings in some patients with pulmonary infiltrates and pleural effusion [7]. Clinically heart failure was not suspected in any case as the cause of pulmonary changes [7].

Hilar and mediastinal lymphadenopathy were seen in 3 patients, which is a novel observation. This is interesting because the respiratory tract is probably the transmission route and the primary site of replication for Puumala virus and other Hantaviruses [21]. Hilar adenopathy is variable in viral diseases, being common in measles pneumonia and infectious mononucleosis but rare with other viral pneumonias [9]. Hilar and mediastinal lymphadenopathy may be seen, usually accompanied by pulmonary parenchymal involvement, and not uncommonly by pleural effusions [27]. In the other study mediastinal lymphadenopathy may also associate with subacute congestive heart failure [28]. In the present study, all three patients having adenopathy had pleural effusion, and two of them had also pericardial fluid. Thus the pathogenesis of adenopathy may be related to Puumala virus-induced capillary leakage and overall fluid overload.

However, our study has some limitations. The number of patients was small and the interval between chest radiographs and CT examinations was rather long. Due to limited number of patients no significant difference in reading was expected and therefore we used consensus reading. The multislice-CT scanner was not used and the CT slices were thick. Further, the most severe oliguric phase of the NE disease did not coincide optimally with the time of CT examination. In the future a study with higher number of patients and more precise correlation of lung HRCT findings with patients' clinical findings could show, if pathological HRCT findings are caused by capillary leakage due to virus-associated endothelial damage or by fluid volume overload induced by ARF.

5. Conclusion

Almost every NE patient showed lung parenchymal abnormalities in HRCT. The most common findings of lung involvement in NE can be defined as accumulation of pleural fluid and atelectasis and intralobular and interlobular septal thickening, most profusely in the lower parts of the lung. As a novel finding, lymphadenopathy was seen in the minority, probably as a consequence of capillary leakage and overall fluid overload. Based on this HRCT study and our previous chest radiograph studies, [7,8] lung parenchymal findings can be taken not to be disease-specific in NE, and HRCT is useful only for scientific purposes. Hantavirus infection should be considered as one possible differential diagnosis of patients who present with acute febrile illness and ARF of an unknown origin and with nonspecific radiologic findings.

Conflict of interest

The authors have no conflict of interest.

Acknowledgement

This work was supported by the Competitive Research Funding of the Pirkanmaa Hospital District.

References

- [1] Vapalahti O, Mustonen J, Lundkvist A, Henttonen H, Plyusnin A, Vaheeri A. Hantavirus infections in Europe. *Lancet Infect Dis* 2003;3:653–61.
- [2] Brummer-Korvenkontio M, Vaheeri A, Hovi T, et al. Nephropathia epidemica: detection of antigen in bank voles and serological diagnosis of human infection. *J Infect Dis* 1980;141:131–4.
- [3] Mustonen J, Brummer-Korvenkontio M, Hedman K, Pasternack A, Pietilä K, Vaheeri A. Nephropathia epidemica in Finland: a retrospective study of 126 cases. *Scand J Infect Dis* 1994;26:7–13.
- [4] Lähdevirta J. Nephropathia epidemica in Finland: a clinical, histological and epidemiological study. *Ann Clin Res Suppl* 1971;3:1–154, 8.
- [5] Van Ypersele de Strihou C, Mery JP. Hantavirus-related acute interstitial nephritis in western Europe expansion of a world-wide zoonosis. *Q J Med* 1989;73:941–50.
- [6] Linderholm M, Billström Å, Settergren B, Tärnvik A. Pulmonary involvement in nephropathia epidemica as demonstrated by computed tomography. *Infection* 1992;20:263–6.
- [7] Kanerva M, Paakkala A, Mustonen J, Paakkala T, Lahtela J, Pasternack A. Pulmonary involvement in nephropathia epidemica: radiological findings and their clinical correlations. *Clin Nephrol* 1996;46:369–78.
- [8] Paakkala A, Lempinen L, Paakkala T, Huhtala H, Mustonen J. Medical imaging in nephropathia epidemica and their clinical correlations. *Eur J Intern Med* 2004;15:284–90.
- [9] Hansell DM, Armstrong P, Lynch DA, McAdams HP. *Imaging of Diseases of the Chest*. fourth ed. Elsevier Mosby; 2005. pp. 253–254.
- [10] Clement J, Colson P, McKenna P. Hantavirus pulmonary syndrome in New England and Europe. *N Engl J Med* 1994;331:545–6.
- [11] Launay D, Thomas CH, Fleury D, et al. Pulmonary-renal syndrome due to hemorrhagic fever with renal syndrome: an unusual manifestation of Puumala virus infection in France. *Clin Nephrol* 2003;59:297–300.
- [12] Fakhrai N, Mueller-Mang C, El-Rabadi K, Böhmig GA, Herold CJ. Puumala virus infection: radiological findings. *J Thorac Imaging* 2010; 24; in press.
- [13] Nichol ST, Spiropoulou CF, Morzunov S, et al. Genetic identification of a hantavirus associated with an outbreak of acute respiratory illness. *Science* 1993;262:914–7.
- [14] Duchin JS, Koster FT, Peters JC, et al. Hantavirus Study Group Hantavirus pulmonary syndrome: a clinical description of 17 patients with newly recognized disease. *N Engl J Med* 1994;330:949–55.
- [15] Ketai LH, Williamson MR, Telepak RJ, et al. Hantavirus pulmonary syndrome: radiographic findings in 16 patients. *Radiology* 1994;191:665–8.
- [16] Boroja M, Barrie JR, Raymond GS. Radiographic findings in 20 patients with Hantavirus pulmonary syndrome correlated with clinical outcome. *AJR* 2002;178:159–63.
- [17] Gasparetto EL, Davaus T, Escuissato DL, Marchiori E. Hantavirus pulmonary syndrome: high-resolution CT findings in one patient. *Br J Radiol* 2007;80:21–3.
- [18] Goncalves FG, Jovem CL, Isac VM, Neves PO. High-resolution computed tomography findings in Hantavirus pulmonary syndrome. *J Thorac Imaging* 2010;25:33–5.
- [19] Vapalahti O, Lundkvist A, Kallio-Kokko H, et al. Antigen properties and diagnostic potential of Puumala virus nucleocapsid protein expressed in insect cells. *J Clin Microbiol* 1996;34:119–25.
- [20] Linderholm M. Nephropathia epidemica. Pathogenetic mechanisms with special reference to pulmonary involvement. Academic Thesis, University of Umeå, Sweden. 1997, 1–64.
- [21] Kanerva M, Mustonen J, Vaheeri A. Pathogenesis of Puumala and other Hantavirus infections. *Rev Med Virol* 1998;8:67–86.
- [22] Conte P, Heitzman ER, Markarian B. Viral pneumonia Roentgen pathological correlations. *Radiology* 1970;95:267–72.
- [23] Temonen M, Vapalahti O, Holthöfer H, et al. Susceptibility of human cells to Puumala virus infection. *J Gen Virol* 1993;74:515–8.
- [24] Collins JD, Burwell D, Furmanski S, Lorber P, Steckel RJ. Minimal detectable pleural effusion. A roentgen pathology model. *Radiology* 1972;105:51–3.
- [25] Thulkar S, Sharma S, Srivastava DN, Sharma SK, Berry M, Pandey RM. Sonographic findings in grade III dengue hemorrhagic fever in adults. *J Clin Ultrasound* 2000;1:34–7.
- [26] Mäkelä S, Kokkonen L, Ala-Houhala I, et al. More than half of the patients with acute Puumala hantavirus infection have abnormal cardiac findings. *Scand J Infect Dis* 2009;41:57–62.
- [27] Limpert J, MacMahon H, Variakojis D. Angioimmunoblastic lymphadenopathy: clinical and radiological features. *Radiology* 1984;152:27–30.
- [28] Chabbert V, Canevet G, Baixas C, et al. Mediastinal lymphadenopathy in congestive heart failure: a sequential CT evaluation with clinical and echocardiographic correlations. *Eur Radiol* 2004;14:881–9.